The actin-related p41ARC subunit contributes to p21-activated kinase-1 (PAK1)–mediated glucose uptake into skeletal muscle cells

Received for publication, June 9, 2017, and in revised form, September 21, 2017 Published, Papers in Press, September 25, 2017, DOI 10.1074/jbc.M117.801340

Ragadeepthi Tunduguru[‡§], Jing Zhang[§], Arianne Aslamy[§¶], Vishal A. Salunkhe[§], Joseph T. Brozinick[‖], Jeffrey S. Elmendorf[‡¶], and Debbie C. Thurmond[‡§¶1]

From the Departments of [‡]Biochemistry and Molecular Biology and [¶]Cellular and Integrative Physiology, Center for Diabetes and Metabolic Diseases,Indiana University School of Medicine, Indianapolis, Indiana 46202, the [§]Department of Molecular and Cellular Endocrinology, Diabetes and Metabolism Research Institute and Beckman Research Institute of the City of Hope, Duarte, California 91010, and [‖]Eli Lilly and Company, Indianapolis, Indiana 46285

Edited by Jeffrey E. Pessin

Defects in translocation of the glucose transporter GLUT4 are associated with peripheral insulin resistance, preclinical diabetes, and progression to type 2 diabetes. GLUT4 recruitment to the plasma membrane of skeletal muscle cells requires F-actin remodeling. Insulin signaling in muscle requires p21-activated kinase-1 (PAK1), whose downstream signaling triggers actin remodeling, which promotes GLUT4 vesicle translocation and glucose uptake into skeletal muscle cells. Actin remodeling is a cyclic process, and although PAK1 is known to initiate changes to the cortical actin-binding protein cofilin to stimulate the depolymerizing arm of the cycle, how PAK1 might trigger the polymerizing arm of the cycle remains unresolved. Toward this, we investigated whether PAK1 contributes to the mechanisms involving the actin-binding and -polymerizing proteins neural Wiskott-Aldrich syndrome protein (N-WASP), cortactin, and ARP2/3 subunits. We found that the actin-polymerizing ARP2/3 subunit p41ARC is a PAK1 substrate in skeletal muscle cells. Moreover, co-immunoprecipitation experiments revealed that insulin stimulates p41ARC phosphorylation and increases its association with N-WASP coordinately with the associations of N-WASP with cortactin and actin. Importantly, all of these associations were ablated by the PAK inhibitor IPA3, suggesting that PAK1 activation lies upstream of these actin-polymerizing complexes. Using the N-WASP inhibitor wiskostatin, we further demonstrated that N-WASP is required for localized F-actin polymerization, GLUT4 vesicle translocation, and glucose uptake. These results expand the model of insulin-stimulated glucose uptake in skeletal muscle cells by implicating p41ARC as a new component of the insulin-signaling cascade and connecting PAK1 signaling to N-WASP-cortactin–mediated actin polymerization and GLUT4 vesicle translocation.

This study was supported by National Institutes of Health Grants DK067912 and DK102233 (to D. C. T.), American Heart Association Grants 15PRE21970002 (to R. T.) and 17POST33661194 (to J. Z.), American Diabetes Association Grant 1-15-BS-053 (to J. S. E.), and a gift from the Ruth and Robert Lanman Endowment (to D. C. T.). The authors declare that they have no conflicts of interest with the contents of this article. The content is solely the responsibility of the authors and does not necessarily represent the official views of the National Institutes of Health.

This article contains supplemental Movies 1 and 2.

[1] To whom correspondence should be addressed: Dept. of Molecular and Cellular Endocrinology, Diabetes and Metabolism Research Institute and Beckman Research Institute of City of Hope, 1500 E. Duarte Rd., Duarte, CA 91010. Tel.: 626-218-0190; E-mail: dthurmond@coh.org.

Insulin stimulates glucose uptake into skeletal muscle and adipose tissue by mobilizing intracellular vesicles containing the glucose transporter GLUT4 to the plasma membrane (PM)[2] (reviewed in Refs. 1, 2). Integration of GLUT4 into the PM facilitates glucose entry into the cell. Skeletal muscle accounts for ~80% of insulin-dependent postprandial glucose uptake (3, 4); skeletal muscle insulin resistance contributes to the development of type 2 diabetes (5). Hence, targeting mechanisms to promote insulin-stimulated GLUT4 vesicle mobilization provides a means to restore insulin sensitivity.

Skeletal muscle cells respond to insulin via the presence of insulin receptors at the cell surface, triggering the canonical insulin signaling pathway: insulin binds to the insulin receptor to induce autophosphorylation, which in turn induces tyrosine phosphorylation of insulin receptor substrate and, subsequently, phosphorylation of PI3K (reviewed in Refs. 6, 7). In skeletal muscle, the pathway downstream of PI3K bifurcates into two parallel and independent arms: one arm leads to phosphorylation of the protein kinase B/AKT, and the second arm leads to the activation of the monomeric small GTPase protein Rac1 (8). Rac1 activation evokes phosphorylation of its effector protein, p21-activated kinase-1 (PAK1) (9, 10). Although the events downstream of the AKT arm of insulin signaling are well documented in these glucose uptake mechanisms (11–16), the events downstream of PAK1 remain incompletely determined.

In humans, insulin-induced PAK1 activation is impaired in skeletal muscle in acute (intralipid infusion) and chronic (high-fat diet–induced obesity and type 2 diabetes) insulin-resistant states, implicating the requirement of PAK1 for insulin-dependent glucose uptake/disposal (9). Whole-body PAK1 knock-out mice replicate these findings (17), as did use of the group 1 PAK inhibitor IPA3, providing evidence for PAK1 involvement in actin remodeling to promote GLUT4 vesicle translocation (18). Stimulus-induced actin cytoskeletal remodeling requires the action of multiple actin-binding proteins that coordinate spatial and temporal polymerization with depolymerization events (19). In a non-canonical signaling mechanism, PAK1 was found

[2] The abbreviations used are: PM, plasma membrane; N-WASP, neural Wiskott-Aldrich syndrome protein; WISK, wiskostatin; IB, immunoblotting; MEM, minimum Eagle's medium.

to regulate insulin-induced actin remodeling in skeletal muscle cells in a LIM kinase–independent manner, signaling to cofilin (actin severing protein) to initiate actin depolymerization (18, 20). Actin remodeling in skeletal myotubes and myoblasts has been tied to insulin-stimulated localization of GLUT4 to plasma membrane ruffles (21–23).

In some cell types, PAK1 can regulate actin remodeling by phosphorylating p41ARC, a regulatory subunit of the ARP2/3 complex that promotes actin polymerization (24–26). Although ARP2/3 has been implicated as a positive factor in GLUT4 translocation in skeletal muscle cells (20), involvement of p41ARC remains untested. PAK1 is implicated in actin polymerization via its ability to enhance binding of the actin nucleating/polymerization factors cortactin and N-WASP (27). Cortactin is an actin nucleation–promoting factor that mediates the assembly and organization of actin cytoskeletal meshwork (28). Cortactin is required for insulin-induced GLUT4 translocation and glucose uptake in skeletal muscle cells (29). In Hep2b clonal hepatocytes, phosphorylation of cortactin by PAK1 specifically at Ser-405 and Ser-418 increased the affinity of cortactin for a known enhancer of actin polymerization, neuronal Wiskott-Aldrich syndrome protein (N-WASP) (27). Overexpression of a dominant-negative N-WASP protein was used to first implicate these factors and actin polymerization in GLUT4 translocation (30). However, whether N-WASP is required for insulin-induced actin remodeling or glucose uptake in skeletal muscle cells has not been investigated. Hence, PAK1 may signal through p41ARC→ARP2/3 or cortactin→N-WASP or both pathways to evoke actin polymerization to support GLUT4 vesicle mobilization and glucose uptake in skeletal muscle cells.

To explore these possible pathways, we have used chemical inhibitors, live-cell imaging, and immunoprecipitation studies to discern the insulin-induced changes in protein–protein complexes concurrent with changes in glucose uptake and GLUT4 translocation. N-WASP was determined to be essential as a mediator of PAK1 in insulin-induced actin remodeling and GLUT4 translocation and to be associated with cortactin. Further, PAK1 activation was required for its association with p41ARC and actin in skeletal muscle cells. Altogether, these findings elucidate new elements of the insulin signaling pathway downstream of Rac1–PAK1 in skeletal muscle that dictate cortical F-actin remodeling and subsequent mobilization of GLUT4 vesicles and fusion to the cell surface.

Results

p41ARC serves as a PAK1 substrate and N-WASP binding partner in insulin-stimulated skeletal muscle cells

In a cancer cell line, PAK1 phosphorylates the Arp2/3 subunit p41ARC (24). Testing this in L6-GLUT4myc myoblasts, we show that insulin stimulated the phosphorylation of p41ARC$^{Thr\text{-}21}$ (Fig. 1*A*) and that this was decreased in lysates from IPA3-treated cells (Fig. 1*B*). N-WASP co-immunoprecipitation studies revealed the interaction of p41ARC with N-WASP in these same myoblast lysates; the abundance of these complexes increased in response to insulin stimulation (Fig. 1*C*). This insulin-stimulated increase in p41ARC–N-WASP association was abolished by pretreatment of myoblasts with the PAK inhibitor IPA3. These data implicate PAK1 as an upstream activator of p41ARC in the insulin signaling cascade.

N-WASP is required for insulin-stimulated GLUT4 vesicle translocation and glucose uptake

Deletion of N-WASP is lethal *in vivo*, and its depletion in cultured cells ablates differentiation (31), and, hence, its role in insulin-stimulated skeletal myotube glucose uptake has remained undetermined. Circumventing this issue, we employed a specific inhibitor of N-WASP, wiskostatin (WISK). WISK is an allosteric inhibitor of N-WASP that interacts with a cleft in the regulatory GTPase-binding domain of N-WASP and stabilizes the native autoinhibited conformation (32). Myotubes respond well to insulin in glucose uptake assays, although they have limited use in live-cell imaging–based assays or assays requiring large amounts of protein (co-immunoprecipitations). Therefore, multiple dosages of WISK were initially tested in myoblasts to determine whether any effects on insulin-induced GLUT4 translocation to the PM were apparent. Insulin induced mobilization of GLUT4 from the intracellular compartments to the plasma membrane of L6-GLUT4myc myoblasts, and this was ablated by 10 μM WISK (Fig. 2, *A* and *B*). WISK also inhibited insulin-stimulated glucose uptake into L6-GLUT4myc myotubes (Fig. 2*C*). WISK used acutely and at this low concentration avoided the reported side effect of decreasing cellular ATP levels (33); levels four times above this dose clearly evoked ATP depletion (Fig. 2*D*). Cell viability was also assessed, with the 10 μM WISK dosage being without effect (Fig. 2*E*). These data reveal a requirement for N-WASP in insulin-stimulated GLUT4 vesicle translocation and glucose uptake in L6 myoblasts and myotubes, respectively.

N-WASP regulates insulin-induced localized F-actin remodeling

To determine the requirement for N-WASP signaling in the process of F-actin remodeling in skeletal muscle cells, live-cell imaging of L6 myoblasts harboring the LifeAct-GFP biosensor was performed, as described previously (18). LifeAct is a 17-residue peptide from the actin-binding protein Abp140 linked to the N terminus of GFP to form LifeAct-GFP, binding specifically to F-actin in live cells without adversely affecting F-actin dynamics (34). Insulin-stimulated changes in actin polymerization in single cells of L6 myoblasts were captured over a period of 10 min, showing localized actin remodeling within 5–6 min of insulin addition in multiple cells within the field (supplemental Movie 1; a representative cell is shown in Fig. 3*A*, vehicle (*Veh*), *arrows* denote sites of remodeling). Addition of 10 μM WISK fully ablated insulin-induced actin remodeling (supplemental Movie 2 and Fig. 3*A*, *WISK*). WISK did not alter global actin cytoskeletal changes because the F:G-actin ratio remained similar compared with vehicle-treated cells (Fig. 3, *B* and *C*). Cells from the same passages that were treated with phalloidin (polymerizer) showed the expected F-actin content of ≥75%, validating that our F:G-actin ratios fell within the dynamic range of the assay according to the established parameters of the manufacturer. Furthermore, insulin did not evoke global changes to F:G-actin ratios, supporting the prevailing concept

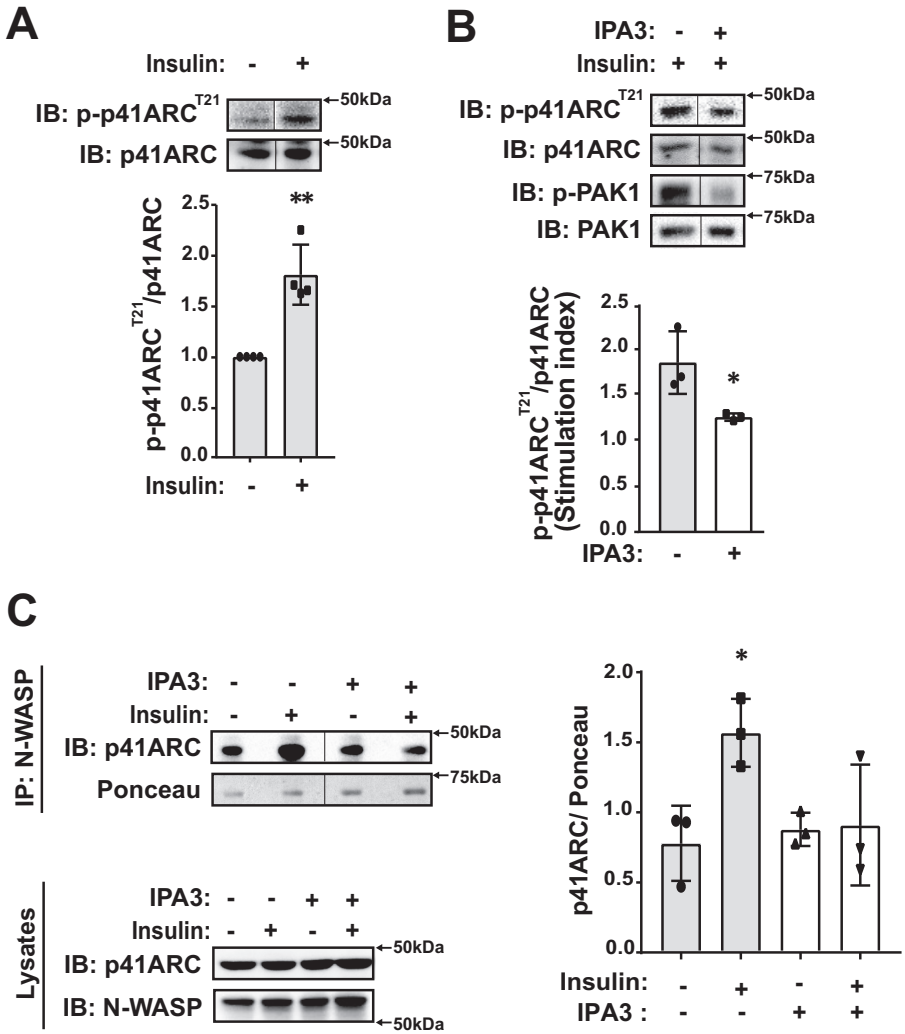

Figure 1. An insulin-dependent interaction of p41ARC with N-WASP is regulated by PAK1. *A* and *B*, L6-GLUT4myc myoblasts were pretreated with vehicle (DMSO) or 25 μM IPA3 for 50 min and stimulated with 100 nM insulin for an additional 10 min. Whole-cell lysates of L6-GLUT4myc myoblasts were analyzed for phosphorylated (p)-p41ARC$^{Thr\text{-}21}$, p41-ARC, PAK1, and p-PAK1/2$^{Thr\text{-}423/402}$ (the p-PAK1 band migrates at 68 kDa) levels. The means ± S.D. from at least three independent sets of cell lysates are shown in the bar graph. *, $p < 0.05$; **, $p < 0.01$. *Black vertical lines* between lanes indicate splicing of lanes from within the same gel exposures. *C*, the whole-cell lysates from above were then immunoprecipitated (*IP*) with N-WASP antibody, and coimmunoprecipitated p41ARC was determined by immunoblotting (IB). The ratio of p41ARC/Ponceau S staining of the same blot was quantified, and the means ± S.D. from three independent sets of cell lysates were determined. *, $p < 0.05$.

in the field that insulin induces localized and not global remodeling of actin. These data suggest that N-WASP is required for localized insulin-stimulated actin remodeling to support GLUT4 vesicle translocation in skeletal muscle cells.

N-WASP interaction with actin and cortactin in response to insulin requires PAK activation

To determine whether PAK1 activity might be linked to actin polymerization in skeletal muscle cells, vehicle- or IPA3-treated myoblasts left unstimulated or stimulated with insulin were used in immunoprecipitation studies. Indeed, immunoprecipitation of N-WASP revealed a 6-fold increase in association of actin with N-WASP in response to insulin stimulation in vehicle-treated L6 myoblasts (Fig. 4*A*); this interaction was significantly reduced in cells treated with IPA3. The actions of insulin and IPA3 to activate and inhibit PAK1 activation, respectively, were validated in each independent experiment using a phospho-specific PAK1/2 antibody. The p-PAK1/2 antibody recognized a 68-kDa band corresponding to the molecular mass of PAK1 that increased upon insulin stimulation and was suppressed by IPA3 (Fig. 4*B*); this was normalized for PAK1 content to quantify the proportion of insulin-stimulated PAK1 activation. A prior study showed PAK2 to be dispensable for insulin-stimulated GLUT4 translocation in L6-GLUT4myc myoblasts (18). Similar to WISK inhibition, IPA3-mediated inhibition had no global effects on the F:G-actin ratio (Fig. 4*C*).

Insulin-stimulated GLUT4 vesicles in muscle and fat cells traffic to the t-SNARE protein Syntaxin 4 (STX4) at the PM for docking and fusion (35–37), and STX4 is noted for its unusual ability to interact both directly and indirectly with F-actin (but not with G-actin) (38, 39). Hence, we questioned whether PAK1 oversight of localized cortical F-actin polymerization would impact STX4 activation at the PM. Testing this, IPA3-treated L6 cells failed to show insulin-stimulated activation of STX4 (Fig. 4*D*). Being similar to that of cells treated with the actin

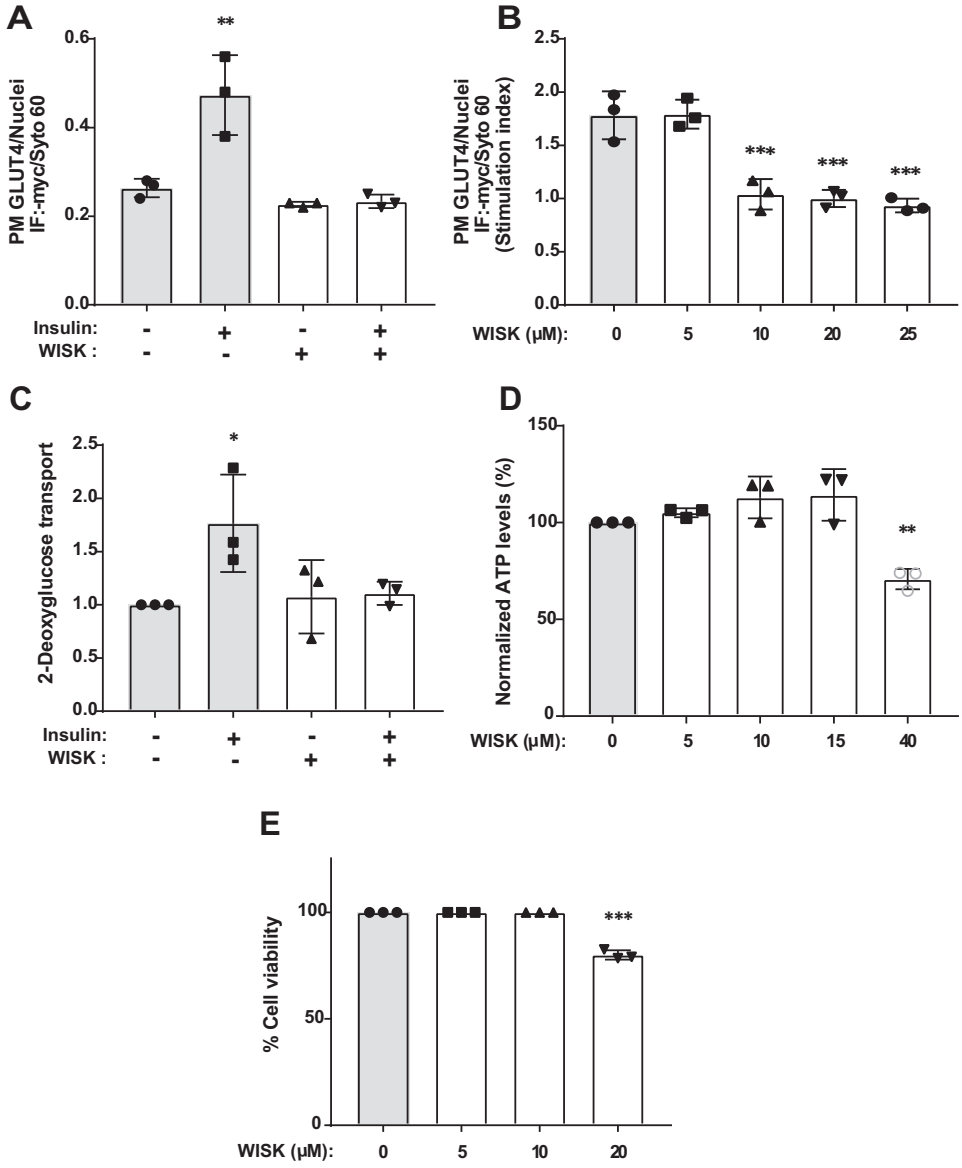

Figure 2. N-WASP inhibition blunts insulin-stimulated glucose uptake and GLUT4 translocation. *A*, L6-GLUT4myc myoblasts were treated with vehicle (DMSO) or 10 μM WISK and stimulated with 100 nM insulin for 20 min simultaneously. Cells were fixed and left unpermeabilized for labeling with anti-myc antibody. The immunofluorescent intensity of cell surface GLUT4 was normalized to the nucleic acid staining dye Syto 60. Values are means ± S.D. from three independent sets of cells. **, $p < 0.01$. *B*, L6-GLUT4myc myoblasts were treated with 0, 5, 10, 20, or 25 μM WISK together with 100 nM insulin for a total of 20 min. Cells were fixed and left unpermeabilized for labeling with anti-myc antibody. The immunofluorescent intensity of cell surface GLUT4 was normalized to the nucleic acid staining dye Syto 60. Values are means ± S.D. from three independent sets of cells. ***, $p < 0.001$. *C*, L6-GLUT4myc myotubes were used for 2-deoxyglucose uptake assays. Values are means ± S.D. from three independent sets of cells. *, $p < 0.05$. *D* and *E*, L6-GLUT4myc myoblasts were treated with DMSO or WISK, and the cellular ATP levels and percentage of viable cells were determined, respectively. Values are means ± S.D. from three independent sets of cells. **, $p < 0.01$; ***, $p < 0.001$.

depolymerizing agent Latrunculin B, these data are consistent with the concept that a link between F-actin and STX4 may be important for insulin-stimulated promotion of the GLUT4 docking/fusion process. Moreover, these data support the notion of insulin-stimulated PAK1 activation fostering the association.

To interrogate the role of PAK1 in the interaction of N-WASP and cortactin in myoblasts, cells were transfected with pGFP–N-WASP, stimulated with or without insulin, and the resulting cell lysates were used in anti-GFP immunoprecipitation reactions. Although the GFP–N-WASP protein was equivalently immunoprecipitated from the different lysates (IB: N-WASP), cortactin was co-immunoprecipitated in ~2-fold greater quantities from insulin-stimulated cells, and this increase was attenuated in cells pretreated with IPA3 (Fig. 5*A*). Cortactin levels in the L6 myoblast lysates were slightly reduced only under the insulin-stimulated condition, although this was not seen in primary muscle homogenates (data not shown). Inhibition of N-WASP by WISK was without effect upon AKT activation (Fig. 5*B*). Similar to the effect of IPA3 and LatB, N-WASP inhibition diminished the insulin-stimulated activation of STX4 (Fig. 5*C*).

Discussion

In this study, we report the existence of new signaling elements downstream of PAK1 that regulate the localized cortical F-actin polymerization arm of the actin remodeling process.

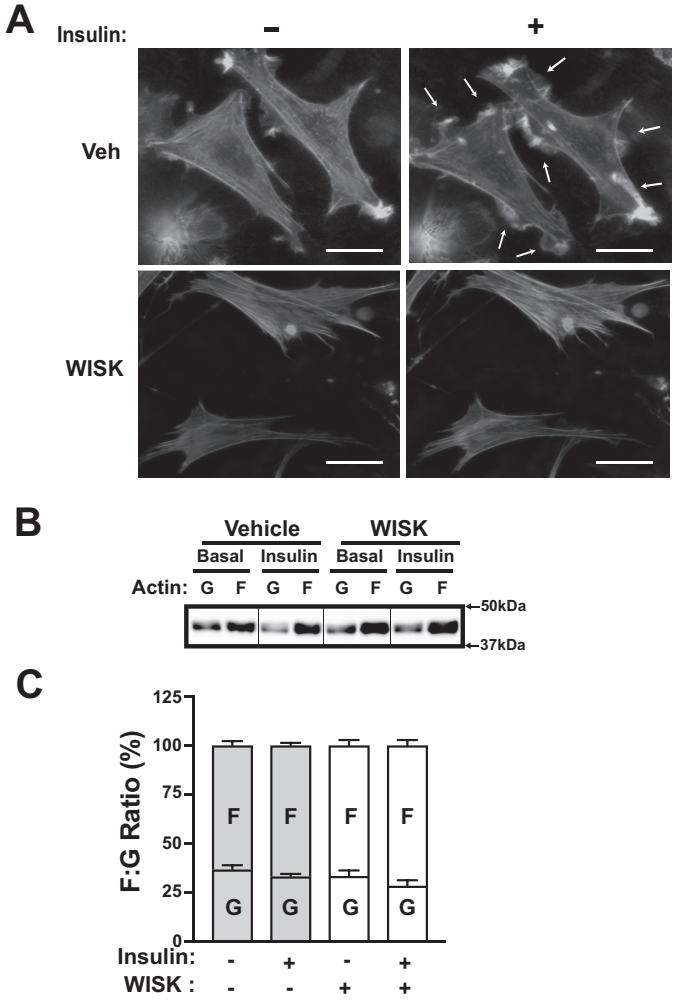

Figure 3. Insulin-stimulated F-actin remodeling requires N-WASP activation. *A*, L6-GLUT4myc myoblasts transfected to express the F-actin binding LifeAct-GFP biosensor were pretreated with vehicle (*Veh*, DMSO) or 10 μM WISK for 10 min, and live-cell confocal imaging was initiated. F-actin remodeling was monitored every minute from 1 min prior to insulin addition to 10 min after insulin addition. *Arrows* indicate sites of F-actin remodeling. At least 20 GFP-positive cells were live-imaged, with >10 treated with WISK, from three independent passages of L6 cells. *Scale bar* = 100 μM. *B*, F- and G-actin from L6-GLUT4myc myoblasts treated with vehicle (DMSO) or 10 μM WISK, left unstimulated (*Basal*), or stimulated with 100 nM insulin for 20 min were resolved by SDS-PAGE for immunoblotting using anti-actin. A representative blot showing the F:G-actin ratio is calculated as a percent of total per sample. *C*, quantitative bar graph representation of the F:G-actin ratio from three independent passages of L6 cells. $p > 0.05$ for all comparisons.

We show that, upon insulin stimulation, PAK1 phosphorylates p41ARC and regulates p41ARC interactions with N-WASP coordinate with the associations of N-WASP with cortactin and actin. Because all of these associations were ablated by inactivation of PAK1, it is likely that PAK1 activation is a proximal step in the process of the formation of these actin-polymerizing complexes. Furthermore, the requirement for N-WASP in localized F-actin polymerization/ruffling and for GLUT4 vesicle translocation and glucose uptake was demonstrated using the N-WASP inhibitor wiskostatin. These results expand the model of insulin-stimulated glucose uptake in skeletal muscle cells by implicating p41ARC as a new component of the insulin-signaling cascade and connecting PAK1 signaling to N-WASP-cortactin–mediated actin polymerization and GLUT4 vesicle translocation.

This is the first report of p41ARC serving as a downstream effector of PAK1 signaling in skeletal muscle cells. PAK1 has been shown to phosphorylate p41ARC$^{\text{Thr-21}}$ *in vitro*, in MCF-7 cancer cells upon EGF stimulation (24, 26), and in melanoma cells (25). p41ARC is one of two principle ARP2/3 subunits, the other and more commonly used subunit being ARPC1A (40). However, to the best of our knowledge, there are no reports of ARPC1A linkage to PAK1. Further supporting the concept of p41ARC in actin polymerization and remodeling, a recent study has demonstrated that p41ARC can be bound and stabilized by cortactin and that this promotes actin assembly and the formation of long actin tails in HeLa cells (41). This adds a new twist to efforts to hamper cellular PAK1 signaling, efforts that would impair a positive and necessary node in a process vital to the maintenance of glucose homeostasis. Having now identified p41ARC as a critical missing link between the insulin signaling and the polymerizing aspect of F-actin remodeling in skeletal muscle cells, future studies detailing the molecular mechanisms will be important to identify ways to improve insulin-stimulated glucose uptake in insulin-resistant muscle.

Indeed, identifying N-WASP as a p41ARC binding partner also provides a novel aspect to the canonical insulin signaling cascade in skeletal muscle cells. Our data concur with a prior study implicating N-WASP in GLUT4 translocation in 3T3L1 adipocytes (30) using a dominant-negative N-WASP mutant. WISK-mediated inhibition of N-WASP activation rapidly and thoroughly abolished insulin-induced cortical actin remodeling and decreased insulin-stimulated GLUT4 translocation in skeletal muscle cells. WISK inhibited these events during the insulin-stimulation period; no lengthy pre-treatment was required to halt these signaling events, being effective at a low dosage that neither diminished ATP levels or cell viability. This supports the concept that the activation of N-WASP, and not its synthesis or the synthesis of other proteins, underlies the PAK1-mediated cascade requiring N-WASP. Furthermore, that insulin-stimulated AKT phosphorylation remained unchanged in the presence of WISK implicates N-WASP in a parallel pathway, leading to GLUT4 vesicle mobilization in skeletal muscle. An alternative to this would be that N-WASP acts downstream of AKT; this has not been demonstrated to date in any cell type to the best of our knowledge. This is consistent with data using inhibitors of PAK1 and Rac1 and the notion that a Rac1→PAK1 signaling pathway occurs independent of/in parallel to the established AKT signaling pathway in skeletal muscle cells.

Insulin stimulation increased the association of N-WASP with cortactin in L6 myoblasts, and this was completely abolished by IPA3, indicating a role for PAK1 in regulating this interaction. A potential mechanism could involve PAK1 phosphorylation of cortactin$^{\text{Ser-408,Ser-4118}}$, as it does in Hep2b cells, coincident with increased association of cortactin-N-WASP and increased localized actin polymerization (27). However, PAK1-mediated phosphorylation of cortactin$^{\text{Ser-113}}$ as seen in smooth muscle cells inhibits cortactin–actin association and F-actin polymerization (44). Alternatively, Rac1 may activate N-WASP, as has been reported to occur *in vitro* (42), in tandem

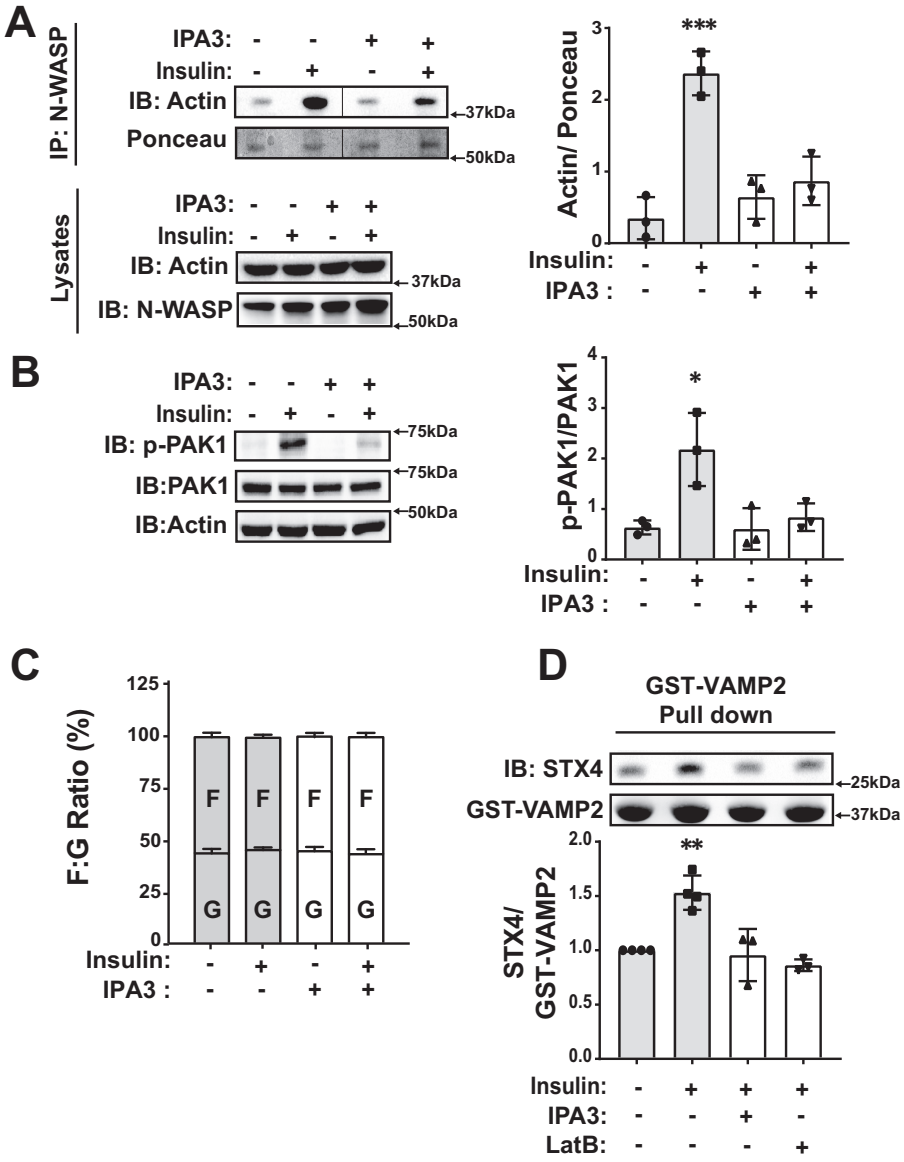

Figure 4. Inhibition of PAK1 activation decreases the insulin-stimulated association of Actin with N-WASP. *A*, L6-GLUT4myc myoblasts were pretreated with vehicle (DMSO) or 25 μM IPA3 for 50 min and stimulated with 100 nM insulin for an additional 10 min. Whole-cell lysates were subjected to immunoprecipitation (*IP*) with anti-N-WASP antibody, and precipitated proteins were resolved using SDS-PAGE for immunoblot analyses. Actin levels were normalized for loading using Ponceau S staining of the same blot section in each of three independent sets of cell lysates. Values represent the means ± S.D. ***, $p < 0.001$. *B*, whole-cell lysates from the experiments in *A* were analyzed for p-PAK1/2$^{Thr\text{-}423,Thr\text{-}402}$ (p-PAK1 band at 68 kDa shown) and total PAK1 protein levels. The pPAK1 band (68 kDa) was quantified as a fraction of corresponding total PAK1 in each of three independent co-immunoprecipitations. *, $p < 0.05$. *C*, L6-GLUT4myc myoblasts pretreated with vehicle (DMSO) or 25 μM IPA3 were stimulated with 100 nM insulin for 10 min. F- and G-actin were separated by ultracentrifugation and analyzed on SDS-PAGE. Data represent the means ± S.D. of three sets of cell F:G-actin ratios. $p > 0.05$. *D*, L6-GLUT4myc myoblasts pretreated with vehicle, 25 μM IPA3, or 10 μM Latrunculin B (*LatB*) were stimulated with 100 nM insulin for 5 min and harvested for use in STX4 activation assays, as described under "Experimental Procedures." Values are the means ± S.D. of three independent experiments using at least two independent batches of recombinant GST-VAMP2 protein. **, $p < 0.01$.

with PAK1 regulation of cortactin. Cortactin and N-WASP can synergistically activate the ARP2/3 complex via cortactin binding to ARP3 and N-WASP binding to p41ARC and ARP2 (43). Although both scenarios involve cortactin, and cortactin is reportedly required for insulin-induced GLUT4 translocation and glucose uptake in skeletal muscle cells (29), validation of the role of cortactin in primary skeletal muscle will require new antibodies; at present, the requisite antibodies are not commercially available. In addition, although IPA3 and WISK are considered highly selective for their targets, it remains possible that either drug could impact Rac1 activation via an unknown feedback signal; this requires testing over a thorough time course given the cyclic nature of the remodeling process. Regarding IPA3, our studies showed it to reduce binding of N-WASP to p41ARC and cortactin back to basal levels, yet there remained a small and statistically insignificant amount of residual N-WASP-actin binding. Although PAK-independent signaling could be responsible, IPA3 only inhibits unphosphorylated PAK1 (45). Given that our data showed a residual level of insulin-stimulated p-PAK1 in cell lysates used for the N-WASP-actin co-immunoprecipitation, this could account for the residual insulin-stimulated N-WASP–actin binding observed.

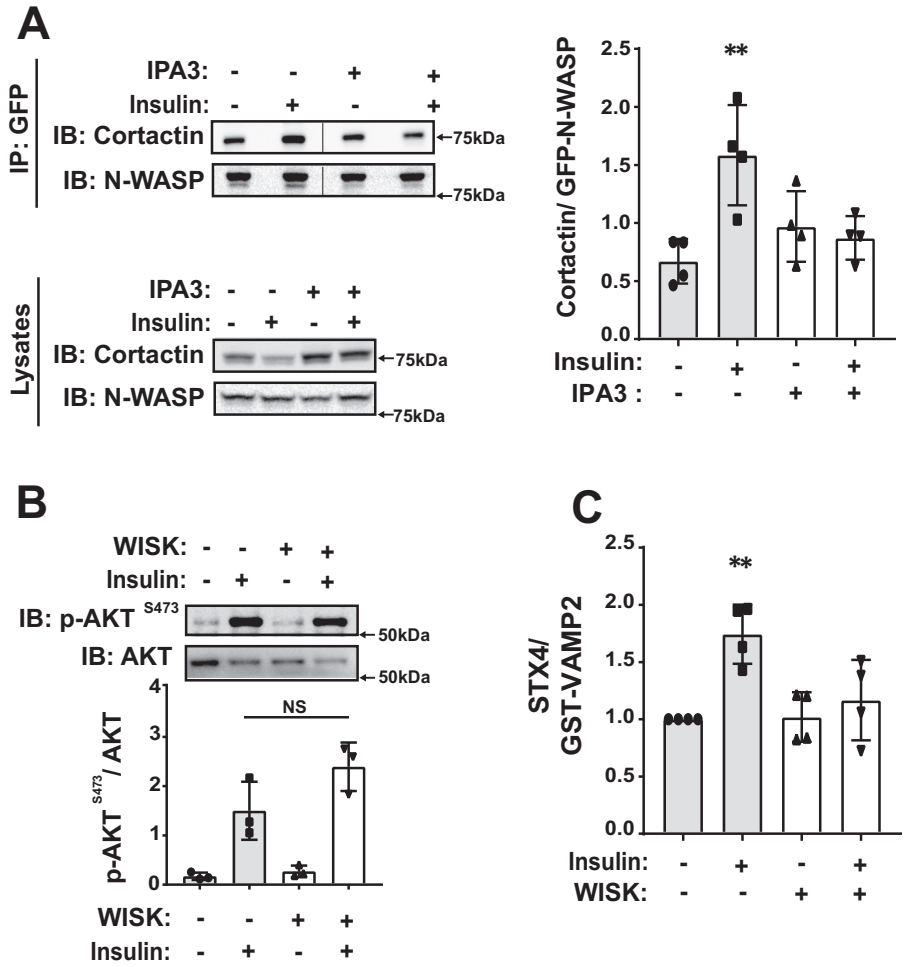

Figure 5. A PAK1-regulated, insulin-dependent N-WASP–cortactin interaction. *A*, L6-GLUT4myc myoblasts were transfected to express GFP-tagged N-WASP and, after 48 h, pretreated with vehicle (DMSO) or 25 μM IPA3 for 50 min and stimulated with 100 nM insulin for an additional 10 min. Whole-cell lysates were immunoprecipitated (*IP*) with anti-GFP antibody, and coimmunoprecipitated cortactin was determined by IB. *Bars* represent the means ± S.D. of four independent sets of L6 cells. **, $p < 0.01$. *B*, AKT activation in cells treated with or without WISK, representative of three independent sets of cells. $p > 0.05$/not significant (*NS*). *C*, L6-GLUT4myc myoblasts treated with vehicle or 10 μM WISK were stimulated with 100 nM insulin for 5 min and harvested for use in STX4 activation assays, as described under "Experimental Procedures." Values are the means ± S.D. of four independent experiments using at least two independent batches of recombinant GST-VAMP2 protein. **, $p < 0.01$.

This study contributes to the body of knowledge on actin remodeling in skeletal muscle cells by revealing the involvement of phospho-p41ARC–N-WASP–cortactin interactions. However, this signaling cascade, overseeing the process of localized F-actin polymerization, must be balanced with respect to the actin depolymerization signaling cascade, involving cofilin and slingshot 1 (SSH1) (20). Indeed, the products of depolymerization are G-actin monomers, and these monomers are the building blocks of F-actin filaments. Conceptually, it is by compilation of these opposing arms of the actin remodeling cycle that the spatial and temporal rearrangement of cortical F-actin creates tracks for the GLUT4 vesicles to move along to the cell surface STX4-based SNARE docking and fusion sites. Future studies are warranted to visualize these events in live skeletal muscle cells, as can currently be seen in 3T3L1 adipocytes (46), and discern the detailed mechanisms regarding the ability of insulin to orchestrate the balance favoring actin polymerization and actin depolymerization.

Altogether, our new findings place PAK1 as a central regulator of insulin sensitivity to maintain glucose homeostasis, and a reduction in PAK1 signaling/abundance might be a potential risk factor for prediabetes susceptibility. Because PAK1 is such a central "hub" for activities in actin remodeling in many cell types, identification of the primary pathways emanating from PAK1 in skeletal muscle will be important as a means to intervene beyond any PAK1 mutations or deficiencies. This will also circumvent any issues raised by retrospective samples associating PAK1 hyperactivation with various types of cancer (47). Hence, efforts to restore PAK1 signaling leading to GLUT4 vesicle exocytosis in skeletal muscle have the potential to reinstate insulin sensitivity in prediabetic and type 2 diabetic individuals.

Experimental procedures

Materials

Rat L6 GLUT4-myc skeletal muscle cells expressing c-myc–tagged GLUT4 protein were purchased from Kerafast and cultured as described previously (48). MEM-α medium was purchased from Invitrogen. Porcine insulin, DMSO, WISK, and rabbit anti-actin antibody were purchased from Sigma. The

LifeAct-GFP plasmid was kindly provided by Dr. Louis Philipson (University of Chicago (49)). The recombinant GFP-tagged N-WASP plasmid was kindly provided by Dr. Susan Gunst (Indiana University) (50). The F:G-actin ratio kit was obtained from Cytoskeleton (Denver, CO). IPA3, protein G+ beads, and mouse anti-c-myc antibody were purchased from Santa Cruz Biotechnology (catalog no. sc-40, Santa Cruz, CA). Rabbit anti-phospho-PAK1$^{Thr-423}$/phospho-PAK2$^{Thr-402}$ (catalog no. 2601), rabbit anti-PAK1 (catalog no. 2602), rabbit anti-N-WASP (catalog no. 4848), and rabbit anti-cortactin (catalog no. 3502) antibodies were obtained from Cell Signaling Technology (Danvers, MA). Rabbit anti-p41ARC antibody (catalog no. AP4321) and rabbit anti-phospho-p41ARC^{Thr-21} (catalog no. AP4351) were obtained from ECM Biosciences (Versailles, KY). Rabbit polyclonal GFP antibody conjugated to Sepharose beads was purchased from Abcam (Cambridge, MA, catalog no. ab69314). Fetal bovine serum and goat anti-mouse horseradish peroxidase secondary antibody were obtained from Thermo Fisher Scientific (Rockford, IL). Goat anti-rabbit horseradish peroxidase secondary antibody was purchased from Bio-Rad. ECL, ECL Prime, and SuperSignal^{TM} Femto were purchased from GE Healthcare and Pierce, respectively.

Cell culture and viability

L6-GLUT4myc myoblasts were grown as monolayers in MEM-α medium supplemented with 10% fetal bovine serum and 1% (v/v) antibiotic–antimycotic solution. L6-GLUT4-myc myoblasts at 40% confluency were differentiated into myotubes by incubation in MEM-α medium containing 2% fetal bovine serum (51, 52). For all studies involving IPA3, L6-GLUT4-myc myoblasts (~ 90% confluency) were preincubated in serum-free medium for 2 h, with IPA3 added for the times indicated in the figures just prior to insulin stimulation (100 nM). With the exception of the live-cell imaging studies, all experiments using WISK were preincubated in serum-free medium for 2 h, with WISK and insulin (100 nM) added simultaneously. Cell viability was assessed using trypan blue staining (Gibco). Cells were harvested in 1% Nonidet P-40 lysis buffer containing 25 mM HEPES (pH 7.4), 1% Nonidet P-40, 10% glycerol, 50 mM sodium fluoride, 10 mM sodium pyrophosphate, 137 mM NaCl, 1 mM sodium vanadate, 1 mM phenylmethylsulfonyl fluoride, 10 μg/ml aprotinin, 1 μg/ml pepstatin, and 5 μg/ml leupeptin and cleared of insoluble material by centrifugation at 13,000 $\times$ *g* for 10 min at 4 °C. The cleared lysate was used for immunoblot analyses.

Cell surface GLUT4myc detection

Cell surface GLUT4myc detection was performed as described previously (53). Briefly, L6-GLUT4-myc myoblasts were incubated in serum-free medium containing WISK (10 μM) or vehicle (DMSO) for 20 min together with insulin (100 nM) at 37 °C. Cells were then fixed with 4% paraformaldehyde in PBS for 20 min at room temperature, blocked in Odyssey blocking buffer (LI-COR Biosciences, Lincoln, NE) for 1 h at room temperature, and incubated with mouse anti-Myc antibody (1:100) overnight at 4 °C. Cells were extensively washed with PBS and then incubated with infrared-conjugated secondary antibody for 1 h at room temperature. The immunofluorescence intensity of the IR-conjugated secondary antibody was quantified using the Odyssey CLx infrared imaging system (LI-COR Biosciences), and data were normalized to Syto 60 (Invitrogen), a red fluorescent nucleic acid stain.

2-deoxyglucose uptake assay

The 2-deoxyglucose uptake assay was performed as described previously (54). Briefly, L6-GLUT4*myc* myotubes were preincubated in serum-free FCB buffer (125 mM NaCl, 5 mM KCl, 1.8 mM $CaCl_2$, 2.6 mM $MgSO_4$, 25 mM HEPES, 2 mM pyruvate, and 2% BSA) for 30 min, and WISK or vehicle was added with insulin for a total period of 20 min. Glucose uptake was initiated by addition of 2-deoxy[1,2,-^{3}H]glucose (0.055 μCi/μl), and uptake was terminated after 5 min by four quick washes with ice-cold PBS followed by addition of 250 μl of 1 N NaOH for quantitation of [^{3}H] using liquid scintillation. Data were normalized for variability in protein concentration, as determined by Bradford assay.

Cellular ATP levels

L6-GLUT4myc myoblasts were incubated with serum-free medium for 2 h and treated with DMSO (vehicle) or different concentrations of wiskostatin for a total of 20 min. The ATP concentration from these cells was determined by following the manufacturers protocol (ATPlite luminescence assay system, PerkinElmer Life Sciences, 6016943) and using a Synergy^{TM} HTX multimode microplate reader (BioTek).

Immunoblotting

Proteins in cell lysates were resolved using 10% SDS-PAGE and transferred to PVDF or nitrocellulose membranes for immunoblotting. Immunoreactive bands were visualized using ECL or ECL Prime reagents and imaged using a Chemi-Doc Touch gel documentation system (Bio-Rad).

Live-cell imaging

L6-GLUT4myc myoblasts were seeded on MatTek glass-bottom culture dishes at a density of 300,000 cells/35-mm dish. At ~40% confluency, cells were transfected with the LifeAct-GFP plasmid using Effectene transfection reagent (Qiagen, Valencia, CA). Live-cell imaging was performed on cells 48 h post-transfection. Briefly, on the day of the experiment, the cells were preincubated in serum-free KRPH buffer (120 mM NaCl, 2.5 mM KCl, 20 mM HEPES, 1.2 mM $MgSO_4$, 1 mM NaH_2PO_4, and 2 mM $CaCl_2$) supplemented with 5 mM D-glucose for 3 h, and then DMSO or WISK was added 10 min before addition of 100 nM insulin for live-cell imaging. LifeAct-GFP imaging was performed on a Keyence imaging system outfitted with a $\times$63 objective and a sample chamber with controlled temperature, humidity, and CO_2. Images were captured every 60 s starting 1 min before addition of insulin and continued until 10 min after the addition of insulin. Representative cells from each treatment group were selected from the real-time movies (supplemental Movies 1 and 2).

Immunoprecipitation

L6-GLUT4myc myoblasts transfected to overexpress GFP–N-WASP protein were incubated in serum-free medium for

2 h, pretreated with IPA3 for 50 min, and stimulated with 100 nM insulin for 10 min. Whole-cell lysate (2.5 mg protein) was immunoprecipitated by incubation with 40 μl of rabbit polyclonal GFP antibody conjugated to Sepharose beads (Abcam, catalog no. ab69314) overnight. Non-transfected cell co-immunoprecipitation reactions were conducted similarly using rabbit anti-N-WASP antibody (catalog no. 4848, Cell Signaling Technology), followed by incubation with protein G+ beads for 2 h at 4 °C. Immunoprecipitated proteins were washed three times with lysis buffer and eluted with SDS sampling buffer containing DTT. Eluted proteins were resolved using 10% SDS-PAGE and transferred to PVDF or nitrocellulose membranes for immunoblotting. N-WASP immunoblotting or Ponceau S staining was used to evaluate protein loading.

F:G-actin ratio in L6-GLUT4myc myoblasts

L6-GLUT4myc myoblasts were incubated with serum-free medium for 2 h and treated with DMSO or 10 μM WISK with 100 nM insulin for a total of 20 min. The F:G-actin ratio from the treated cells described above was determined by following the manufacturers protocol (Cytoskeleton).

STX4 activation assay

The GST-VAMP2 protein was generated in *Escherichia coli* and purified by glutathione–agarose affinity chromatography for use in the STX4 accessibility assay. L6 cell lysates were prepared from cells stimulated with insulin with or without IPA3, LatB, or WISK treatment. GST-VAMP2 protein linked to Sepharose beads was combined with 2 mg of each type of L6 myoblast detergent cell lysate for 2 h at 4 °C in 1% Nonidet P-40 lysis buffer, followed by three stringent washes with the lysis buffer. The associated proteins were resolved on 10% SDS-PAGE, followed by their transfer to PVDF membranes for immunoblotting for STX4, as described previously (55).

Statistical analysis

All data were expressed as the mean ± S.D. and assessed by Student's *t* test (only Fig. 1, *A* and *B*) and analysis of variance with a Tukey post-hoc test using GraphPad Prism™ (La Jolla, CA).

Author contributions—R. T. and D. C. T. designed and implemented the study and wrote the paper. R. T. performed all studies, with assistance from J. Z., who performed co-immunoprecipitation experiments; A. A., who performed the STX4 accessibility assays; and V. A. S., who performed the ATP assays and assisted with Keyence live-cell imaging. J. T. B. and J. S. E. contributed to skeletal muscle and L6 cell assay designs and execution. All authors analyzed the results, edited the manuscript, and approved the final version of the manuscript.

Acknowledgments—We thank Dr. Susan Gunst and Dr. Simon Atkinson (Indiana University) for the N-WASP plasmid and sage advice and feedback on this project emanating from the doctoral dissertation of R. T. We also thank Lixuan Tackett, Erika Olson, and Rajakrishnan Veluthakal for technical assistance. The research reported in this publication also includes work performed in the Light Microscopy Core, supported by the NCI, National Institutes of Health under Award P30CA33572.

References

1. Leto, D., and Saltiel, A. R. (2012) Regulation of glucose transport by insulin: traffic control of GLUT4. *Nat. Rev. Mol. Cell Biol.* **13,** 383–396
2. Foley, K., Boguslavsky, S., and Klip, A. (2011) Endocytosis, recycling, and regulated exocytosis of glucose transporter 4. *Biochemistry* **50,** 3048–3061
3. Ferrannini, E., Smith, J. D., Cobelli, C., Toffolo, G., Pilo, A., and DeFronzo, R. A. (1985) Effect of insulin on the distribution and disposition of glucose in man. *J. Clin. Invest.* **76,** 357–364
4. Thiebaud, D., Jacot, E., DeFronzo, R. A., Maeder, E., Jequier, E., and Felber, J. P. (1982) The effect of graded doses of insulin on total glucose uptake, glucose oxidation, and glucose storage in man. *Diabetes* **31,** 957–963
5. DeFronzo, R. A., and Tripathy, D. (2009) Skeletal muscle insulin resistance is the primary defect in type 2 diabetes. *Diabetes Care* **32,** S157-S163
6. De Meyts, P. (2016) in *EndoText* (De Groot, L. J., Chrousos, G., Dungan, K., Feingold, K. R., Grossman, A., Hershman, J. M., Koch, C., Korbonits, M., McLachlan, R., New, M., Purnell, J., Rebar, R., Singer, F., and Vinik, A., eds.) MDText.com, South Dartmouth, MA
7. Ramalingam, L., Oh, E., and Thurmond, D. C. (2013) Novel roles for insulin receptor (IR) in adipocytes and skeletal muscle cells via new and unexpected substrates. *Cell Mol. Life Sci.* **70,** 2815–2834
8. Klip, A., Sun, Y., Chiu, T. T., and Foley, K. P. (2014) Signal transduction meets vesicle traffic: the software and hardware of GLUT4 translocation. *Am. J. Physiol. Cell Physiol.* **306,** C879-C886
9. Sylow, L., Jensen, T. E., Kleinert, M., Højlund, K., Kiens, B., Wojtaszewski, J., Prats, C., Schjerling, P., and Richter, E. A. (2013) Rac1 signaling is required for insulin-stimulated glucose uptake and is dysregulated in insulin-resistant murine and human skeletal muscle. *Diabetes* **62,** 1865–1875
10. Tsakiridis, T., Taha, C., Grinstein, S., and Klip, A. (1996) Insulin activates a p21-activated kinase in muscle cells via phosphatidylinositol 3-kinase. *J. Biol. Chem.* **271,** 19664–19667
11. Chen, S., Wasserman, D. H., MacKintosh, C., and Sakamoto, K. (2011) Mice with AS160/TBC1D4-Thr649Ala knockin mutation are glucose intolerant with reduced insulin sensitivity and altered GLUT4 trafficking. *Cell Metab.* **13,** 68–79
12. Ishikura, S., Bilan, P. J., and Klip, A. (2007) Rabs 8A and 14 are targets of the insulin-regulated Rab-GAP AS160 regulating GLUT4 traffic in muscle cells. *Biochem. Biophys. Res. Commun.* **353,** 1074–1079
13. Kramer, H. F., Witczak, C. A., Taylor, E. B., Fujii, N., Hirshman, M. F., and Goodyear, L. J. (2006) AS160 regulates insulin- and contraction-stimulated glucose uptake in mouse skeletal muscle. *J. Biol. Chem.* **281,** 31478–31485
14. Ishikura, S., and Klip, A. (2008) Muscle cells engage Rab8A and myosin Vb in insulin-dependent GLUT4 translocation. *Am. J. Physiol. Cell Physiol.* **295,** C1016–1025
15. Randhawa, V. K., Ishikura, S., Talior-Volodarsky, I., Cheng, A. W., Patel, N., Hartwig, J. H., and Klip, A. (2008) GLUT4 vesicle recruitment and fusion are differentially regulated by Rac, AS160, and Rab8A in muscle cells. *J. Biol. Chem.* **283,** 27208–27219
16. Sun, Y., Bilan, P. J., Liu, Z., and Klip, A. (2010) Rab8A and Rab13 are activated by insulin and regulate GLUT4 translocation in muscle cells. *Proc. Natl. Acad. Sci. U.S.A.* **107,** 19909–19914
17. Wang, Z., Oh, E., Clapp, D. W., Chernoff, J., and Thurmond, D. C. (2011) Inhibition or ablation of p21-activated kinase (PAK1) disrupts glucose homeostatic mechanisms *in vivo*. *J. Biol. Chem.* **286,** 41359–41367
18. Tunduguru, R., Chiu, T. T., Ramalingam, L., Elmendorf, J. S., Klip, A., and Thurmond, D. C. (2014) Signaling of the p21-activated kinase (PAK1) coordinates insulin-stimulated actin remodeling and glucose uptake in skeletal muscle cells. *Biochem. Pharmacol.* **92,** 380–388
19. Carlier, M. F., Pernier, J., Montaville, P., Shekhar, S., Kühn, S., and Cytoskeleton Dynamics and Motility Group (2015) Control of polarized assembly of actin filaments in cell motility. *Cell Mol. Life Sci.* **72,** 3051–3067
20. Chiu, T. T., Patel, N., Shaw, A. E., Bamburg, J. R., and Klip, A. (2010) Arp2/3- and cofilin-coordinated actin dynamics is required for insulin-mediated GLUT4 translocation to the surface of muscle cells. *Mol. Biol. Cell* **21,** 3529–3539

21. Langlais, P., Dillon, J. L., Mengos, A., Baluch, D. P., Ardebili, R., Miranda, D. N., Xie, X., Heckmann, B. L., Liu, J., and Mandarino, L. J. (2012) Identification of a role for CLASP2 in insulin action. *J. Biol. Chem.* **287,** 39245–39253
22. Khayat, Z. A., Tong, P., Yaworsky, K., Bloch, R. J., and Klip, A. (2000) Insulin-induced actin filament remodeling colocalizes actin with phosphatidylinositol 3-kinase and GLUT4 in L6 myotubes. *J. Cell Sci.* **113,** 279–290
23. Vu, V., Bui, P., Eguchi, M., Xu, A., and Sweeney, G. (2013) Globular adiponectin induces LKB1/AMPK-dependent glucose uptake via actin cytoskeleton remodeling. *J. Mol. Endocrinol.* **51,** 155–165
24. Vadlamudi, R. K., Li, F., Barnes, C. J., Bagheri-Yarmand, R., and Kumar, R. (2004) p41-Arc subunit of human Arp2/3 complex is a p21-activated kinase-1-interacting substrate. *EMBO Rep.* **5,** 154–160
25. Ho, H., Soto Hopkin, A., Kapadia, R., Vasudeva, P., Schilling, J., and Ganesan, A. K. (2013) RhoJ modulates melanoma invasion by altering actin cytoskeletal dynamics. *Pigment Cell Melanoma Res.* **26,** 218–225
26. Kim, Y. B., Shin, Y. J., Roy, A., and Kim, J. H. (2015) The role of the pleckstrin homology domain-containing protein CKIP-1 in activation of p21-activated kinase 1 (PAK1). *J. Biol. Chem.* **290,** 21076–21085
27. Grassart, A., Meas-Yedid, V., Dufour, A., Olivo-Marin, J. C., Dautry-Varsat, A., and Sauvonnet, N. (2010) Pak1 phosphorylation enhances cortactin-N-WASP interaction in clathrin-caveolin-independent endocytosis. *Traffic* **11,** 1079–1091
28. Weed, S. A., and Parsons, J. T. (2001) Cortactin: coupling membrane dynamics to cortical actin assembly. *Oncogene* **20,** 6418–6434
29. Nazari, H., Khaleghian, A., Takahashi, A., Harada, N., Webster, N. J., Nakano, M., Kishi, K., Ebina, Y., and Nakaya, Y. (2011) Cortactin, an actin binding protein, regulates GLUT4 translocation via actin filament remodeling. *Biochemistry* **76,** 1262–1269
30. Jiang, Z. Y., Chawla, A., Bose, A., Way, M., and Czech, M. P. (2002) A phosphatidylinositol 3-kinase-independent insulin signaling pathway to N-WASP/Arp2/3/F-actin required for GLUT4 glucose transporter recycling. *J. Biol. Chem.* **277,** 509–515
31. Gruenbaum-Cohen, Y., Harel, I., Umansky, K. B., Tzahor, E., Snapper, S. B., Shilo, B. Z., and Schejter, E. D. (2012) The actin regulator N-WASp is required for muscle-cell fusion in mice. *Proc. Natl. Acad. Sci. U.S.A.* **109,** 11211–11216
32. Peterson, J. R., Bickford, L. C., Morgan, D., Kim, A. S., Ouerfelli, O., Kirschner, M. W., and Rosen, M. K. (2004) Chemical inhibition of N-WASP by stabilization of a native autoinhibited conformation. *Nat. Struct. Mol. Biol.* **11,** 747–755
33. Guerriero, C. J., and Weisz, O. A. (2007) N-WASP inhibitor wiskostatin nonselectively perturbs membrane transport by decreasing cellular ATP levels. *Am. J. Physiol. Cell Physiol.* **292,** C1562–1566
34. Riedl, J., Crevenna, A. H., Kessenbrock, K., Yu, J. H., Neukirchen, D., Bista, M., Bradke, F., Jenne, D., Holak, T. A., Werb, Z., Sixt, M., and Wedlich-Soldner, R. (2008) Lifeact: a versatile marker to visualize F-actin. *Nat. Methods* **5,** 605–607
35. Cheatham, B., Volchuk, A., Kahn, C. R., Wang, L., Rhodes, C. J., and Klip, A. (1996) Insulin-stimulated translocation of GLUT4 glucose transporters requires SNARE-complex proteins. *Proc. Natl. Acad. Sci. U.S.A.* **93,** 15169–15173
36. Olson, A. L., Knight, J. B., and Pessin, J. E. (1997) Syntaxin 4, VAMP2, and/or VAMP3/cellubrevin are functional target membrane and vesicle SNAP receptors for insulin-stimulated GLUT4 translocation in adipocytes. *Mol. Cell Biol.* **17,** 2425–2435
37. Volchuk, A., Wang, Q., Ewart, H. S., Liu, Z., He, L., Bennett, M. K., and Klip, A. (1996) Syntaxin 4 in 3T3-L1 adipocytes: regulation by insulin and participation in insulin-dependent glucose transport. *Mol. Biol. Cell* **7,** 1075–1082
38. Band, A. M., Ali, H., Vartiainen, M. K., Welti, S., Lappalainen, P., Olkkonen, V. M., and Kuismanen, E. (2002) Endogenous plasma membrane t-SNARE syntaxin 4 is present in rab11 positive endosomal membranes and associates with cortical actin cytoskeleton. *FEBS Lett.* **531,** 513–519
39. Jewell, J. L., Luo, W., Oh, E., Wang, Z., and Thurmond, D. C. (2008) Filamentous actin regulates insulin exocytosis through direct interaction with Syntaxin 4. *J. Biol. Chem.* **283,** 10716–10726
40. Goley, E. D., and Welch, M. D. (2006) The ARP2/3 complex: an actin nucleator comes of age. *Nat. Rev. Mol. Cell Biol.* **7,** 713–726
41. Abella, J. V., Galloni, C., Pernier, J., Barry, D. J., Kjær, S., Carlier, M. F., and Way, M. (2016) Isoform diversity in the Arp2/3 complex determines actin filament dynamics. *Nat. Cell Biol.* **18,** 76–86
42. Tomasevic, N., Jia, Z., Russell, A., Fujii, T., Hartman, J. J., Clancy, S., Wang, M., Beraud, C., Wood, K. W., and Sakowicz, R. (2007) Differential regulation of WASP and N-WASP by Cdc42, Rac1, Nck, and PI(4,5)P2. *Biochemistry* **46,** 3494–3502
43. Higgs, H. N., and Pollard, T. D. (2000) Activation by Cdc42 and PIP(2) of Wiskott-Aldrich syndrome protein (WASp) stimulates actin nucleation by Arp2/3 complex. *J. Cell Biol.* **150,** 1311–1320
44. Webb, B. A., Zhou, S., Eves, R., Shen, L., Jia, L., and Mak, A. S. (2006) Phosphorylation of cortactin by p21-activated kinase. *Arch. Biochem. Biophys.* **456,** 183–193
45. Deacon, S. W., Beeser, A., Fukui, J. A., Rennefahrt, U. E., Myers, C., Chernoff, J., and Peterson, J. R. (2008) An isoform-selective, small-molecule inhibitor targets the autoregulatory mechanism of p21-activated kinase. *Chem. Biol.* **15,** 322–331
46. Lim, C. Y., Bi, X., Wu, D., Kim, J. B., Gunning, P. W., Hong, W., and Han, W. (2015) Tropomodulin3 is a novel Akt2 effector regulating insulin-stimulated GLUT4 exocytosis through cortical actin remodeling. *Nat. Commun.* **6,** 5951
47. Wang, R. A., Zhang, H., Balasenthil, S., Medina, D., and Kumar, R. (2006) PAK1 hyperactivation is sufficient for mammary gland tumor formation. *Oncogene* **25,** 2931–2936
48. Walker, P. S., Ramlal, T., Sarabia, V., Koivisto, U. M., Bilan, P. J., Pessin, J. E., and Klip, A. (1990) Glucose transport activity in L6 muscle cells is regulated by the coordinate control of subcellular glucose transporter distribution, biosynthesis, and mRNA transcription. *J. Biol. Chem.* **265,** 1516–1523
49. Lopez, J. P., Turner, J. R., and Philipson, L. H. (2010) Glucose-induced ERM protein activation and translocation regulates insulin secretion. *Am. J. Physiol. Endocrinol. Metab.* **299,** E772–785
50. Zhang, W., Wu, Y., Du, L., Tang, D. D., and Gunst, S. J. (2005) Activation of the Arp2/3 complex by N-WASp is required for actin polymerization and contraction in smooth muscle. *Am. J. Physiol. Cell Physiol.* **288,** C1145–1160
51. Kanai, F., Nishioka, Y., Hayashi, H., Kamohara, S., Todaka, M., and Ebina, Y. (1993) Direct demonstration of insulin-induced GLUT4 translocation to the surface of intact cells by insertion of a c-myc epitope into an exofacial GLUT4 domain. *J. Biol. Chem.* **268,** 14523–14526
52. Ueyama, A., Yaworsky, K. L., Wang, Q., Ebina, Y., and Klip, A. (1999) GLUT-4myc ectopic expression in L6 myoblasts generates a GLUT-4-specific pool conferring insulin sensitivity. *Am. J. Physiol.* **277,** E572–578
53. Habegger, K. M., Penque, B. A., Sealls, W., Tackett, L., Bell, L. N., Blue, E. K., Gallagher, P. J., Sturek, M., Alloosh, M. A., Steinberg, H. O., Considine, R. V., and Elmendorf, J. S. (2012) Fat-induced membrane cholesterol accrual provokes cortical filamentous actin destabilisation and glucose transport dysfunction in skeletal muscle. *Diabetologia* **55,** 457–467
54. McCarthy, A. M., Spisak, K. O., Brozinick, J. T., and Elmendorf, J. S. (2006) Loss of cortical actin filaments in insulin-resistant skeletal muscle cells impairs GLUT4 vesicle trafficking and glucose transport. *Am. J. Physiol. Cell Physiol.* **291,** C860–868
55. Ramalingam, L., Oh, E., and Thurmond, D. C. (2014) Doc2b enrichment enhances glucose homeostasis in mice via potentiation of insulin secretion and peripheral insulin sensitivity. *Diabetologia* **57,** 1476–1484